

Optimization of laser doping process in crystalline silicon solar cells

Abhishek Sharan^{*‡}, B. Prasad^{**}

*Amorphous Silicon Solar Cell Plant, Bharat Heavy Electricals Limited, BHEL-ASSCP, C/o BHEL House, Siri fort, New Delhi-110049, India

** Amorphous Silicon Solar Cell Plant, Bharat Heavy Electricals Limited, BHEL-ASSCP, C/o BHEL House, Siri fort, New Delhi-110049, India

(abhisheks@bhel.in, bprasad@bhel.in)

[‡]Corresponding Author; Amorphous Silicon Solar Cell Plant, Bharat Heavy Electricals Limited, BHEL-ASSCP, C/o BHEL House, Siri fort, New Delhi-110049, India Tel: +91-124-2579221 Fax: +91-124-2579227, abhisheks@bhel.in

Received: 31.07.2013 Accepted: 22.08.2013

Abstract- A large area selective emitter patterning scheme is developed and reported in the present study that features a single additional step compared to the standard process. Initially, trials are conducted to achieve a uniform base sheet resistance of $100\pm 10 \Omega/\text{sq}$ in p-type c-Si wafers using POCl₃ diffusion on a large area 156 x 156 mm silicon wafers. Thereafter, employing a nanosecond, Q-switched, green laser and phosphosilicate glass layer (PSG) as a dopant source, areas below the front contact fingers are heavily doped while areas between them are kept lowly doped, thus realizing a selective emitter. This study refers to optimization of diffusion parameters to achieve uniform diffusion of base sheet resistance of $100\pm 10 \Omega/\text{sq}$ and optimization of laser parameters for achieving localized regions of high doping to attain selective emitter structure.

Keywords- Laser, Doping, Diffusion, Crystalline silicon solar cell, sheet resistance.

1. Introduction

Low Ohmic contacts to the front side of p-n junction Si solar cells require high doping in the “emitter” (usually the n-type) part of the cell. Unfortunately, high doping goes hand-in-hand with increased Auger recombination and decreased quantum efficiency for short wavelength radiation. The “selective” emitter (SE) concept uses laterally different emitter doping: (i) high doping under the front side metallization for low contact resistance between contact metal and semiconductor interface, (ii) low doping between the contact fingers for a better short wavelength response owing to reduced Auger recombination [1] as well as improved emitter passivation [2,3]. Unfortunately, most SE concepts developed so far in research imply a high process complexity due to the required steps for masking of selective diffusion [4] or emitter

etch back [5]. In essence, these concepts are difficult to implement into industrial production of solar cells. Several different SE approaches for industrial production are currently under development [6,7] or are being transferred to the industry [8].

The present paper refers to optimization of laser parameters for achieving high doping in regions below the front metal contacts employing furnace diffused silicon wafers as the base material. The add-on laser doping increases the doping concentration as well as the emitter depth underneath the contact fingers, thus yielding good Ohmic contacts. The silver metallization is then put exactly over the laser doped regions using high precision screen printer. The laser doping has several advantages over the chemical etching process, conventionally used for achieving selective emitter. These include a dry process, having a high accuracy and fast speed. In the present paper, we have discussed tuning of laser parameters

for laser diffusion of furnace diffused emitter for achieving selectively doped emitter.

2. Experimental

Figure 1 below describes the process sequence for Laser Doped selective emitter solar cell structure for which the starting material is 156 mm x 156 mm in size, 200 μm thick, p-type Czochralski grown wafers. Step 1 textures the wafer surface by a standard, alkaline etching process that produces random pyramids and reduces the optical reflectivity of the surface. Step 2 creates the n-type phosphorus doped emitter together with a phosphosilicate glass (PSG) layer on top by conventional POCl_3 diffusion process. The PSG layer mainly consists of $\text{SiO}_2:\text{P}_2\text{O}_5$ with the ratio of SiO_2 and P_2O_5 depending on the processing time, gas composition, gas flow and diffusion temperature [9]. The sheet resistivity of the wafer is adjusted to lie in the range of $100 \pm 10 \Omega/\text{sq}$. by experimenting with several combinations of the flat zone temperature, pre-diffusion time and the drive-in time.

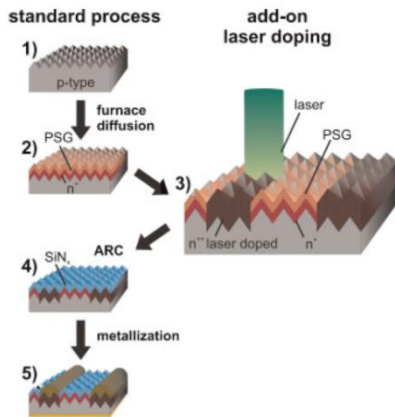
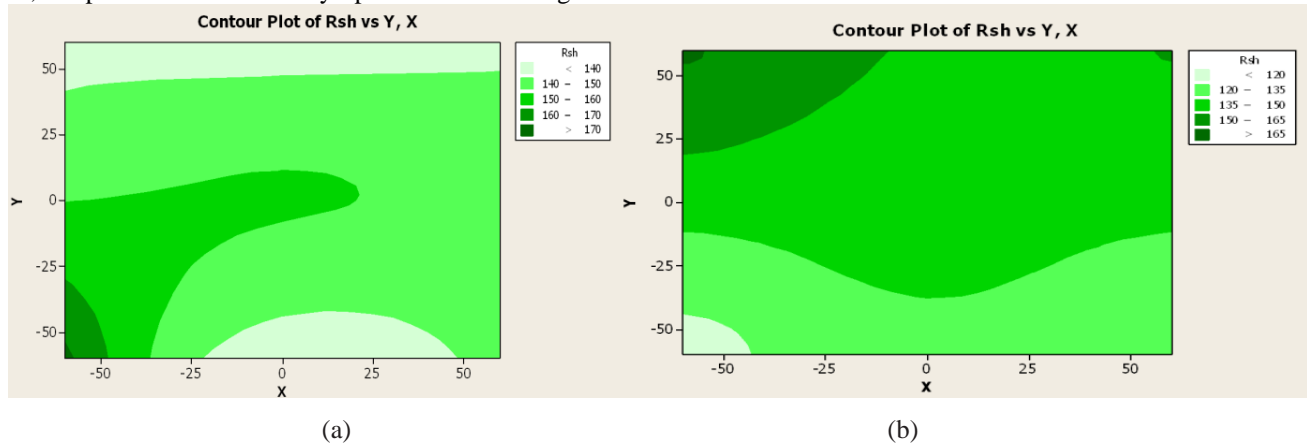


Fig.1. Process flow for laser doped selective emitter solar cells.

In Step 3, laser doping is carried out to create heavily diffused, deep emitter over closely spaced localized regions.



The PSG layer serves as the doping precursor. The laser that is used for laser doping is a nanosecond, green (532 nm), Nd:VO4 laser with a spot size of approximately 25 μm . The laser frequency used is either 50 or 55 kHz at which frequency the laser shows the maximum stability. The laser parameters varied for process optimization of laser doping include laser power (0.2 – 1.2 W), scan speed (500 – 1200 mm/sec), laser shift in transverse direction and number of cycles (1 – 6). To determine the effect of laser doping and its dependence on various factors, the sheet resistance of wafers before and after laser doping are measured and the ratio of the sheet resistances ($R_{\text{sheet after laser doping}}/R_{\text{sheet before laser doping}}$) used as the parameter for determining the effectiveness of laser doping.

In Step 4, Hydrofluoric acid is used to remove the PSG layer and a SiN_x anti reflection coating (ARC) is deposited over the emitter. Before putting the ARC, the wafers are mapped with respect to their sheet resistance using a four probe measurement set up. The cell fabrication process is completed in Step 5 by applying the front and back metal contacts with screen printing and firing. The last process step, however, is beyond the scope of this study.

3. Results and discussions

3.1. Shallow emitter diffusion

Figure 2 depicts the contour plots of resistivity measurements for six different experiments on emitter diffusion as described above. The summary of the results with the process parameters is shown in Table 1. From the figure and the table, it is clear that at the diffusion temperature of 780 $^{\circ}\text{C}$, a pre-deposition time of 45 min and a drive-in time of 25 min yield a mean sheet resistance of 106.1 Ω/sq with a standard deviation of 5.37 Ω/sq . This is the base wafer that is used in our subsequent study of optimization of laser parameters to achieve a target sheet resistance of $40 \pm 10 \Omega/\text{sq}$ after laser diffusion.

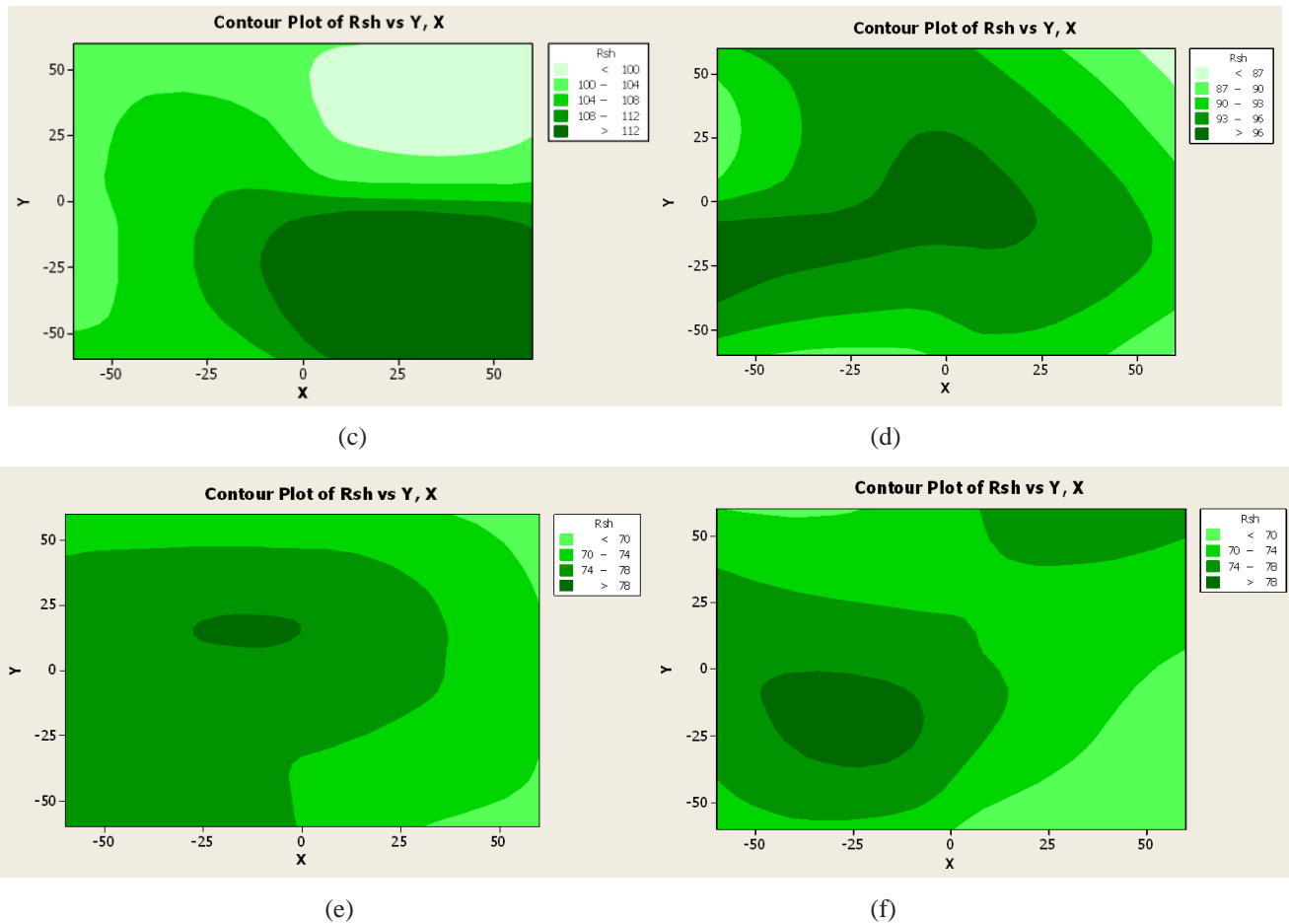


Fig.2. Contour plots of Sheet Resistance for different experiments on emitter diffusion

Table 1. Variation of Rsheet with diffusion parameters

Sl. No.	Diffusion Temp (°C)	Pre Dep Time (minute)	Drive In Time (minute)	Mean Rsheet (Ω/Sq.)	Std Dev (Ω/Sq.)
A	770	45	30	145.3	12.7
B	785	45	20	139.3	19.4
C	780	45	25	106.1	5.37
D	800	45	20	92.3	3.56
E	795	45	30	73.3	3.15
f	800	45	30	72.8	3.21

3.2. Laser Power Optimization

The variation of laser power has a significant effect on emitter doping. This is seen from Fig. 3 where the ratio of sheet resistance of the laser doped region to that of the base

wafer is plotted against the laser power. The plot shows that efficiency of laser doping, shown by a reduction in the ratio of sheet resistances, increases with an increase in the laser power applied. While keeping the other laser parameters constant, this ratio reaches the minimum value at a laser power of 0.3 and 0.4 W and then begins to increase. This suggests that the laser doping is most optimal at 0.3 and 0.4 W.

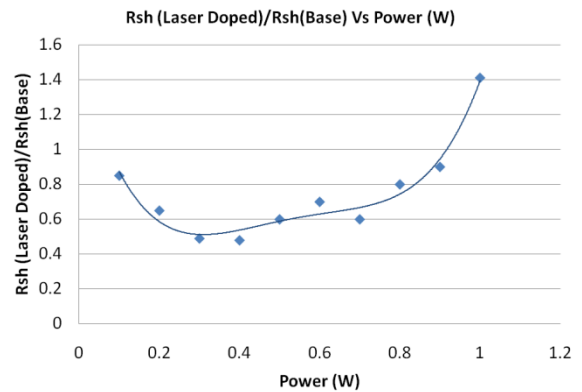


Fig.3. Variation of the ratio of sheet resistances of laser doped region to that of the base wafer vs. laser power

The increase in the ratio of sheet resistances beyond 0.4 W of laser power suggests that phosphorous doping decreases at higher laser powers. At a laser power close to 1.0 W, the sheet resistance of the laser doped region even exceeds that of the

base wafer suggesting ablation of silicon atoms along with phosphorus atoms. This is very well depicted in the SEM images of the samples in Fig.4.

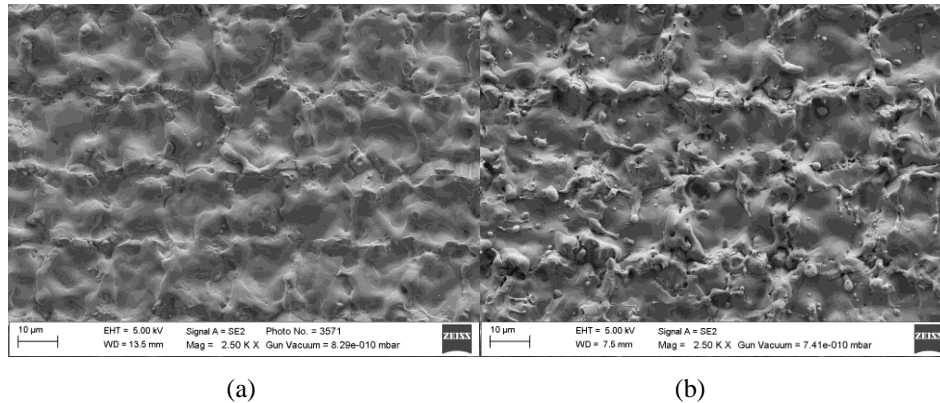


Fig.4. SEM images of silicon wafer after laser doping with laser power of (a) 0.4 W, (b) 0.9 W

3.3. Laser Scan Speed Optimization

The laser in use is a pulsed laser with a spot size of approximately 25 μm. However, as depicted in Fig. 5, the spot size varies a little with the laser power. It is desired that for uniform doping, the consecutive laser pulses sufficiently overlap each other.

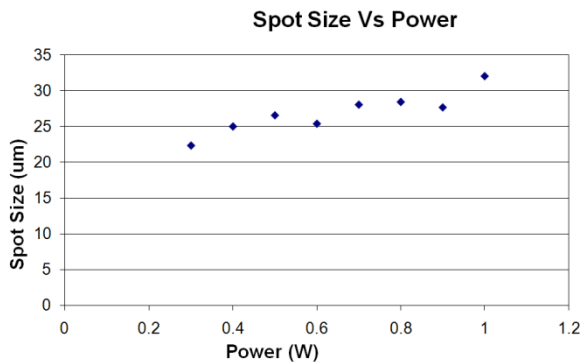


Fig.5. Variation of laser spot size with laser

The overlapping of consecutive laser pulses is dependent on the scan speed of the laser spot and the effect is clearly visible from the SEM images of Fig. 6 where a good overlap of laser pulses at a speed of 800 mm/sec is compared with a no-overlap case at a scan speed of 1200 mm/sec.

This is suggestive of the fact that lower scan speeds are preferred for doping uniformity. However, appearance of visual uniformity alone does not ascertain effective doping. For this, ratio of sheet resistance is plotted against scan speed (Fig 7). It is seen from this plot that lower scan speeds (500-600 mm/sec) are preferred for optimum laser doping.

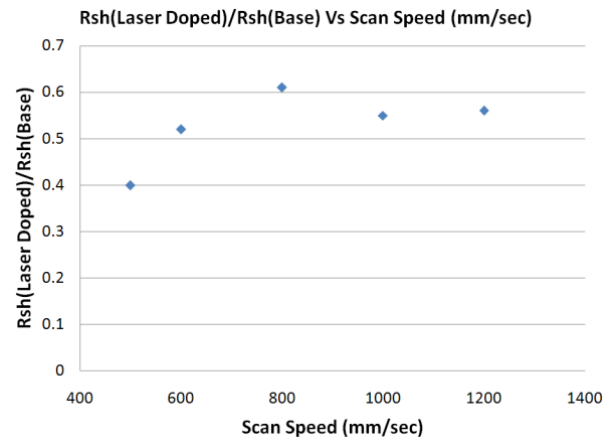
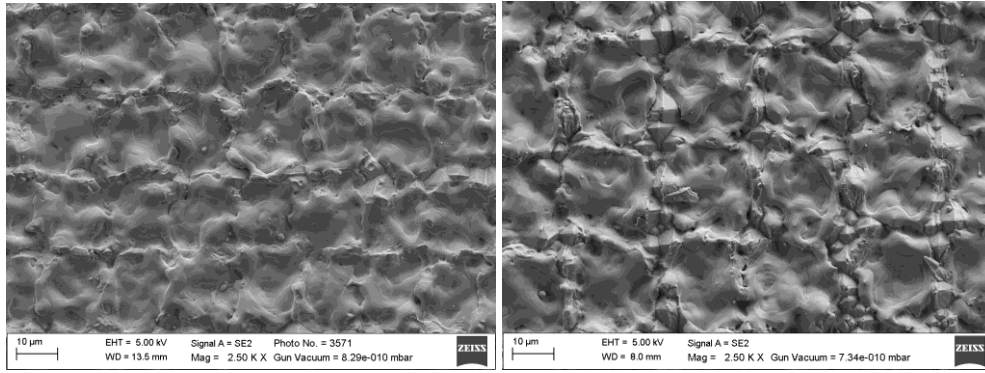


Fig.7. Variation of ratio of sheet resistance of laser doped region to that of base wafer with laser scan speed (laser power of 0.4 W, laser shift of 22 μm in transverse direction & no. of cycles as 1)



Speed = 800 mm/sec
 Speed = 1200 mm/sec
Fig.6. SEM images showing laser pulse overlap at different laser scan speeds

3.4. Laser Shift in transverse direction and no. of cycles:

While optimization of laser scan speed is required to maintain pulse overlap in the horizontal direction, optimization of laser shift in transverse direction is required to maintain pulse overlap in the vertical direction. The plot of the mean of the ratio of sheet resistances obtained from laser doping at

various set of laser parameters at a specific laser shift versus laser shift (in μm) in transverse direction is shown in Fig. 8(a). It is evident from the plot that at 20 μm laser shift the ratio of sheet resistance is higher when compared to laser shifts at 16 μm and 18 μm .

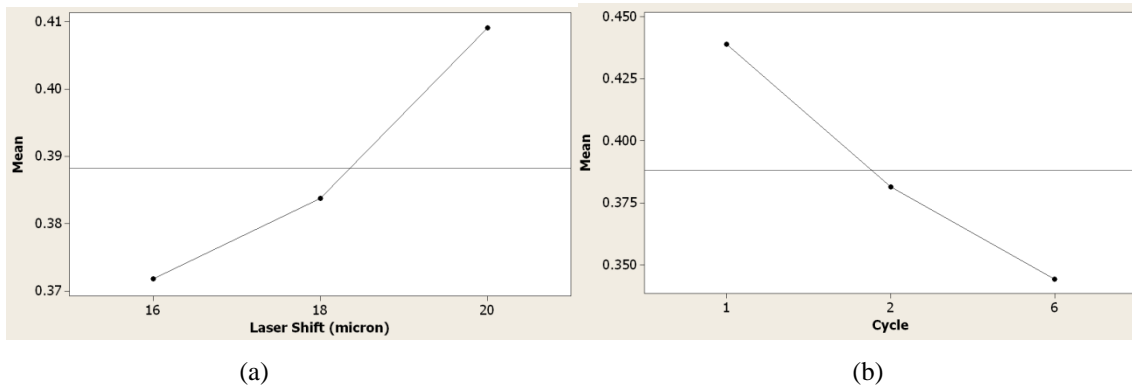


Fig. 8 The effect of laser shift in transverse direction and no. of cycles on laser doping

Fig 8(b) above plots the mean of the ratio of sheet resistance obtained from laser doping at various set of laser parameters repeated a number of times (cycle) Vs the number of repetition of laser doping (cycle). 6 cycles shows a significant reduction in sheet resistance of the samples. However, for industrial processes 6 cycles is not feasible since it a long time and leads to low throughput. Therefore, for industrial processes comprising 1 and 2 cycles are preferred over a 6-cycle process.

Having obtained the optimized ranges of laser power, scan speed, laser shift in transverse direction and no. of cycles, from the above described experiments, studies are carried out on a number of combinations of these laser parameters. From the measurement of sheet resistances, the following four sets of laser parameters show the optimal results with the minimum ratio of sheet resistances, which are feasible to be incorporated into production, as shown in Table 2.

Table 2. Laser Parameters corresponding to the desired value the ratio of sheet resistances in the Laser Doped region to laser undoped region

Sl.No.	Laser Power (W)	Laser Speed (mm/sec)	Scan	Laser shift in transverse direction (μm)	No. of cycles	Rsh(Laser Doped)/Rsh(Base)
1	0.4	500		18	2	0.32
2	0.4	500		20	2	0.32
3	0.3	500		16	2	0.33
4	0.4	600		16	2	0.33

4. Conclusion

The study described above, optimizes the POCl₃ diffusion process for shallow emitter, of sheet resistance value $100 \pm 10 \Omega/\text{sq}$, to be used for making laser doped selective emitter solar cells. Diffusion temperature of 780°C , pre deposition time of 45 min and drive in time of 25 min have been found to give emitters of sheet resistance value of $106 \Omega/\text{sq}$ with a standard deviation of $5.37 \Omega/\text{sq}$.

The study also includes scanning of various laser parameters involved in laser doping and reveals the set of laser parameters giving minimum ratio of sheet resistances in the laser doped and laser undoped region. A minimum ratio of sheet resistance in laser doped and laser undoped region of 0.32-0.35 have been obtained on a base wafer of sheet resistance $\sim 106 \Omega/\text{sq}$, which is much below the target ratio of 0.40. Such selectively doped emitter is expected to give a high efficiency solar cell.

Acknowledgements

Authors are grateful to the BHEL management and staff for providing constant support and encouragement during the course of this work and finally for permitting publication of the results of the study.

References

- [1] Kerr MJ, Cuevas A. General parameterization of Auger recombination in crystalline silicon. *Applied Physics Letters* 2002; 91: 2473–2480. 10.1063/1.1432476.
- [2] Kerr MJ, Schmidt J, Cuevas A, Bultman JH. Surface recombination velocity of phosphorus-diffused silicon solar cell emitters passivated with plasma enhanced chemical vapor deposited silicon nitride and thermal silicon oxide. *Journal of Applied Physics* 2001; 89: 3821–3826. 10.1063/1.1350633.
- [3] Zhao J, Wang A, Green MA. 24.5% efficiency silicon PERT cells on MCZ substrates and 24.7% efficiency PERL cells on FZ substrates. *Progress in Photovoltaics: Research and Applications* 1999; 7: 471–474. 10.1002/(SICI)1099-159X(199911/12)7:6<471::AID-PIP298>3.0.CO;2-7.
- [4] Engelhart P, Hermann S, Neubert T, Plagwitz H, Grischke R, Meyer R, Klug U, Schoonderbeek A, Stute U, Brendel R. Laser ablation of SiO₂ for locally contacted Si solar cells with ultrashort pulses. *Progress in Photovoltaics: Research and Applications* 2007; 15: 521–527. 10.1002/pip.758.
- [5] Szlufcik J, Elgamel HE, Ghannam M, Nijs J, Mertens R. Simple integral screenprinting process for selective emitter polycrystalline silicon solar cells. *Applied Physics Letter* 1991; 59: 1583–1584. 10.1063/1.106291.
- [6] Hopman S, Fell A, Mayer K, Fleischmann C, Drew K, Kray D, Granek F. Study on laser parameters for silicon solar cells with LCP selective emitters. *Proceedings of the 24th European photovoltaic solar energy conference*, edited by: W. C. Sinke, H. A. Ossenbrink, and P. Helm (WIP, Munich, Germany, 2009), 1072.
- [7] Lauer mann T, Dastgheib-Shirazi A, Book F, Raabe B, Hahn G, Haverkamp H, Habermann D, Demberger C, Schmid C. InSECT: an inline selective emitter concept with high efficiencies at competitive process costs improved with inkjet masking technology. *Proceedings of the 24th European photovoltaic solar energy conference*, edited by: W. C. Sinke, H. A. Ossenbrink, and P. Helm (WIP, Munich, Germany, 2009), 1767.
- [8] Shi Z, Wenham S, Ji J. Mass production of the innovative PLUTO solar cell technology. *Proceedings of the 34th IEEE photovoltaic specialists conference*, Philadelphia, USA, edited by: (IEEE, New York, USA, 2009), 1922.
- [9] Kooi E. Formation and composition of surface layers and solubility limits of phosphorus during diffusion in silicon. *Journal of the Electrochemical Society* 1964; 111: 1383–1387.